This is a repository copy of *The world's first high voltage GaN-on-Diamond power semiconductor devices*.

The World's First High Voltage GaN-on-Diamond Power Semiconductor Devices

Turar Baltynov, Vineet Unni, and E. M. Sankara Narayanan

Department of Electronic and Electrical Engineering

The University of Sheffield

Sheffield S1 3JD, United Kingdom

Abstract—This paper presents the detailed fabrication method and extensive electrical characterisation results of the first-ever demonstrated high voltage GaN power semiconductor devices on CVD Diamond substrate. Fabricated circular GaN-on-Diamond HEMTs with gate-to-drain drift length of 17 μm and source field plate length of 3 μm show an off-state breakdown voltage of ~ 1100 V. Temperature characterisation of capacitance-voltage characteristics and on-state characteristics provides insight on the temperature dependence of key parameters such as threshold voltage, 2DEG sheet carrier concentration, specific on-state resistance, and drain saturation current in the fabricated devices.

Keywords—AlGaN/GaN HEMT, GaN-on-Diamond, circular HEMT, breakdown voltage, capacitance-voltage.

I.   INTRODUCTION

The evolution of advanced power electronic systems is commonly driven by the requirements for smaller size, lower weight, higher efficiency, higher reliability, and lower costs (Fig. 1) [1]. The most frequently used figure of merit which brings together all these parameters and provides a reliable assessment of the progress of the technology is power

density. The power density of power electronic converters has roughly doubled every decade starting from 1970. The present-day technology is already facing the barriers which could limit the power density of power electronic converters in future (Fig. 2) [1].

AlGaN/GaN high electron mobility transistors (HEMTs) are ideal candidates for use in applications with requirements of very high power densities [2]. However, due to poor thermal properties of commonly used starting substrate materials for GaN epitaxial growth (such as Sapphire, Silicon), the usable power densities are limited and the peak operational capability of AlGaN/GaN HEMTs remains unachieved. In order to attain reliable operation and harness the true performance of GaN devices, improved thermal management is necessary [3]. CVD Diamond with its high room-temperature thermal conductivity that is almost 3 to 10 times higher than even thermally conductive substrates such as Silicon Carbide (SiC) could emerge as the ideal substrate option to address the heat transfer issues and aid the development of power electronics with extremely high reliability and power densities. This area of research is gaining focus and reports evaluating integration of Diamond and GaN for device technologies have been published [4, 5]. It has already been shown through simulation and experimental demonstration that GaN-on-Diamond platform can significantly outperform GaN-on-SiC platform for Radio Frequency (RF) applications by reducing thermal resistance and thereby increasing power density [3, 6, 7]. Fig. 3 shows that with GaN-on-Diamond wafers, a nearly threefold improvement in RF power density could be achieved for a given channel temperature when compared to GaN-on-SiC [8]. It should be noted that most of the work which has been accomplished on GaN-on-Diamond till date has been primarily focussed on RF devices.

In this paper, the device fabrication method and detailed electrical characterisation results through evaluation of standard forward and reverse current-voltage (IV) characteristics, capacitance-voltage (CV) characteristics as well as temperature

characterisation results of high voltage AlGaN/GaN HEMTs on CVD Diamond substrates are discussed. The AlGaN/GaN epitaxy used in this work was originally designed and optimised for development of RF Power Amplifier devices.

It should be noted that this paper is an enriched version of the article [9] published in the proceedings of ESSDERC'15 with additional material on the structural details and electrical characteristics of bidirectional GaN HEMTs on Diamond substrates. The motivation of the presented work has been elaborated with the aid of additional illustrations from published literature. The processing steps for device fabrication have been described in detail with additional data on ohmic contacts and 2DEG channel parameters. Description of the measurement setup used for the characterisation of breakdown voltage and small signal capacitance-voltage characteristics has been added. Metrics quantifying key electrical performance characteristics such as average breakdown field strength, temperature coefficients of - sheet carrier concentration, threshold voltage, specific on-state resistance and drain saturation current - have also been included.

II.   FABRICATION AND DEVICE STRUCTURE

Fig. 4 shows cross-sectional schematic of the epi-layer structure of the GaN-on-Diamond wafer as obtained from Element Six. The epi-wafer consists of 95 μm of CVD Diamond substrate, 53 nm of adhesion layer, 800 nm of undoped GaN buffer layer, 20 nm of $Al_{0.26}GaN_{0.74}N$ barrier layer, 2.5 nm of undoped GaN cap-layer, and 50 nm of SiN layer. Figs. 5 (a)-(c) show cross-sectional schematics of the designed AlGaN/GaN HEMT without field plate (FP), with source field plate (SFP) and bidirectional AlGaN/GaN HEMT respectively. Extensive numerical simulations were carried out using Silvaco ATLAS to optimise the device-design parameters. Following this exercise, a fabrication process-flow (10 Masks) was developed.

Device processing begins with mesa etching for device isolation. This was accomplished by a two-step inductively coupled plasma (ICP) etching of 50 nm of SiN followed by 100 nm of the underlying III-Nitride layers. This was followed by blanket deposition of 100 nm thick SiO_2 layer by plasma enhanced chemical vapor deposition (PECVD). 50 nm of SiN and 100 nm of SiO_2 were then etched from active area of the devices by ICP etching. Source and drain ohmic contact electrodes were formed by thermal evaporation and lift-off in acetone, of Ti/Al/Ni/Au (20/100/45/55 nm) followed by rapid thermal annealing (RTA) at 800 °C for 1 min in N_2 ambient. The area-specific contact resistance estimated by transmission line model (TLM) patterns is ~ 1.2 x 10^{-5} $\Omega.cm^2$ [15]. The contact resistance normalised to width of the TLM structure is 0.94 $\Omega.mm$. The sheet resistance of the two-dimensional electron gas (2DEG) at the AlGaN/GaN interface and transfer length were estimated as 687 $\Omega/\square$ and 1.36 μm respectively. Schottky gate contact was deposited by thermal evaporation of Ni/Au (20/200 nm). This was followed by sequential deposition of SiN (50 nm) and SiO_2 (450 nm) layers using PECVD. SiN and SiO_2 layers were etched from the device-pad regions by reactive ion etching (RIE) and source field plates were formed by thermal evaporation/lift-off of Ti/Au (20/480 nm), followed by additional metallisation of pads with Ti/Au (20/480 nm). Finally, a 1000 nm thick layer of SiO_2 was deposited by PECVD over the entire wafer and subsequently etched using RIE to define the terminal pads of the individual devices. Figs. 6 (a)-(d) show the top view photographs of the fabricated HEMT in circular form (without SFP), HEMT in circular form (with SFP), HEMTs in stripe form (without FP), and bidirectional HEMT respectively.

III.   ELECTRICAL CHARACTERISATION

Off-state Breakdown Voltage

Off-state Breakdown Voltage (BV$_{DSS}$) of the circular devices with and without SFP and with various gate-to-drain separations (L$_{GD}$) was measured under Fluorinert ambient by using a Sony Tektronix 370 programmable curve tracer and a bench-top power supply. The bench-top power supply was used to bias the gate-to-source voltage (V$_{GS}$) of the HEMT at -5V (Threshold Voltage V$_{TH}$ ~ - 3 V). The drain voltage was biased using the curve tracer by sweeping the voltage gradually (pulsed mode) from 0 V to the point of electrical breakdown. A simplified illustration of the setup has been shown in Fig. 7. Fig. 8 depicts the measured breakdown voltage values (destructive) of devices with and without SFP with respect to L$_{GD}$. The BV$_{DSS}$ of devices without SFP and varying L$_{GD}$ changes only slightly ~ 550 - 600 V, which corresponds to the average breakdown field strength of ~ 0.18 MV/cm. The devices with SFP and L$_{GD}$ =13 and 17 μm, show considerably higher BV$_{DSS}$ of ~ 800 V and 1100 V respectively. This corresponds to an average breakdown field strength of ~ 0.72 MV/cm, illustrating the enhanced electric field management achieved with the SFP. It has to be noted that the circular devices fabricated in this work even without SFP still show quite high breakdown voltage which is in agreement with other published results for AlGaN/GaN HEMTs with similar circular/square gate design [10, 11]. Figs. 9 (a)-(b) show top view photographs of the circular AlGaN/GaN HEMTs without and with SFP post breakdown evaluation. The breakdown behavior is destructive and the region corresponding to the breakdown has also been demarcated.

B. Capacitance – Voltage Measurements

Small-signal capacitance – voltage (CV) characteristics were measured using Agilent B1505A semiconductor device analyzer with an in-built multi-frequency capacitance measurement unit (MFCMU). Being wafer-level measurements, phase compensation as well

as open and short corrections were performed on the setup before proceeding with the actual device measurements. Fig. 10 shows CV characteristics (measured at 1 MHz and at various temperatures (25 ^{0}C – 125 ^{0}C)) of a 1.1 kV GaN-on-Diamond HEMT in circular form with gate width (W_G) of ~ 430 μm, gate-to-drain drift length (L_{GD}) = 17 μm, and source field plate length (L_{FP}) = 3 μm. The source terminal of the device was left floating during this measurement. As drain-to-gate voltage (V_D) increases, the two-dimensional electron gas (2DEG) at the AlGaN/GaN heterointerface under the gate electrode is depleted at V_D ~ 3 V corresponding to the threshold voltage of the device (V_{TH} ~ - 3 V). Fig. 11 shows the apparent carrier density (N_{CV}) as extracted from the CV measurement data for this device [12]. The peak of apparent carrier concentration N_{CV} = 2.3e19 cm^{-3} is observed at a depth of ~ 19 nm which also corresponds to the centroid of 2DEG at the AlGaN/GaN heterointerface. It can be observed that as the temperature rises, the capacitance slightly increases and the magnitude of V_{TH} shifts towards higher values. Fig. 12 shows the trend of apparent sheet carrier concentration as well as V_{TH} with respect to temperature. The temperature coefficients for the sheet carrier concentration and V_{TH} are found to be ~ 7 x 10^9 cm^{-2}/ ^{0}C and - 2.8 mV/ ^{0}C respectively. The increase in the sheet carrier concentration can be attributed to thermally generated carriers in bulk-regions of the heterostructure [16].

C.   Forward Current Voltage Characteristics

DC characteristics of the devices were measured using Agilent B1500A semiconductor device analyzer. Fig. 13 shows the output current – voltage (I-V) characteristics of the 1.1 kV GaN-on-Diamond HEMT that was used for the CV measurements. The device shows a drain saturation current of about 14 mA at drain voltage V_{DS} ~ 3 V with gate biased at 0 V. The transfer I-V characteristics of the device at V_{DS} = 1 V have been shown in Fig. 14. The threshold voltage (V_{TH}) of the device is ~ - 3 V as also confirmed by CV measurement.

Fig. 15 shows typical transfer I-V characteristics of the fabricated bidirectional GaN-on-Diamond HEMTs (Fig. 6 (d)) with $W_{G1} = W_{G2} = 50$ µm, $L_{G1D} = L_{G2S} = 17$ µm, and gate length $L_{G1} = L_{G2} = 3$ µm. From the transfer I-V characteristics, it is apparent that the drain current of the device is effectively controlled by Gate-1 (voltage V_{G1S}) in forward direction (current flow from D electrode to S electrode (Fig. 6 (d))) and by Gate-2 (voltage V_{G2D}) in the reverse direction (current flow from S electrode to D electrode (Fig. 6 (d))). The measured threshold voltage is found to be around - 3 V. Fig. 16 shows output I-V characteristics of the bidirectional HEMT. The device has symmetrical characteristics in the both directions.

Fig. 17 shows output I-V characteristics (at $V_{GS} = 0$ V) of the GaN-on-Diamond HEMT in linear form (Fig. 6, c) with $W_G = 50$ µm, $L_{GD} = 11$ µm and gate length $L_G = 3$ µm measured at different temperatures (from - 80 ^{0}C to 90 ^{0}C). The measurement was performed on a TTP4 cryogenic manipulated-probe station. Reduction of the drain current with increasing temperature is apparent. This could be attributed to reduced carrier mobility due to increased collisions/scattering at higher temperatures [13]. Fig. 18 shows the trend of specific on-state resistance ($R_{ON}.A$) (measured at $V_{DS} = 2$ V and $V_{GS} = 0$ V) as well as the drain saturation current I_{DSAT} (at $V_{DS} = 4$ V and $V_{GS} = 0$ V) of the device with respect to temperature. A linear trend has been observed for both parameters with a temperature coefficient of ~ 5.85 µΩ.cm^2/ ^{0}C and - 8.62 µA/ ^{0}C for $R_{ON}.A$ and I_{DSAT} respectively. The increase in $R_{ON}.A$ at high temperatures can be primarily attributed to the degradation of the two-dimensional electron gas (2DEG) mobility [14].

IV.   CONCLUDING REMARKS

This paper reports the device fabrication and detailed electrical characterisation results of AlGaN/GaN HEMTs on CVD Diamond substrate. Fabricated circular AlGaN/GaN

HEMTs with source field plate length of 3 μm and gate-to-drain separation of 17 μm have demonstrated an off-state breakdown voltage of ~ 1100 V. The systematic measurements of output I-V, transfer I-V, off-state breakdown voltage, capacitance – voltage characteristics and temperature characterisation results provide insights on the device performance and temperature dependence of the heterostructure characteristics. The GaN-on-Diamond epi-wafers used here were manufactured in late 2013. Devices reported here represented the first-time that a power switching device has been made with GaN-on-Diamond albeit with epitaxy designed for RF applications. The performance shown here is expected to improve with epitaxy that has been better tailored for power electronic applications.

ACKNOWLEDGEMENT

REFERENCES

[1]   Kolar, Johann W., Uwe Drofenik, Juergen Biela, Marcello L. Heldwein, Hans Ertl, Thomas Friedli, and Simon D. Round. "PWM Converter Power Density Barriers." In Power Conversion Conference-Nagoya, 2007. PCC'07, pp. P-9. IEEE, 2007.

[2]   U. K. Mishra, L. Shen, T. E. Kazior, and Y.-F. Wu, "GaN based RF power devices and amplifiers," Proc. IEEE, vol. 96, no. 2, pp. 287–305, Feb. 2008.

[3]   Dumka, D. C., T. M. Chou, F. Faili, D. Francis, and F. Ejeckam. "AlGaN/GaN HEMTs on Diamond substrate with over 7W/mm output power density at 10 GHz." Electronics Letters 49, no. 20 (2013): 1298-1299.

[4]   Altman, David, Matthew Tyhach, James McClymonds, Samuel Kim, Samuel Graham, Jungwan Cho, Kenneth Goodson et al. "Analysis and characterisation of thermal transport in GaN HEMTs on Diamond substrates." In Thermal and Thermomechanical Phenomena in Electronic Systems (ITherm), 2014 IEEE Intersociety Conference on, pp. 1199-1205. IEEE, 2014.

[5]   Blevins, J. D., G. D. Via, K. Sutherlin, S. Tetlak, B. Poling, R. Gilbert, B. Moore et al. "Recent progress in GaN-on-Diamond device technology." In Proc. CS MANTECH Conf, pp. 105-108. 2014.

[6]   Pomeroy, J., Mirko Bernardoni, Andrei Sarua, A. Manoi, D. C. Dumka, D. M. Fanning, and M. Kuball. "Achieving the Best Thermal Performance for GaN-on-Diamond." In Compound Semiconductor Integrated Circuit Symposium (CSICS), 2013 IEEE, pp. 1-4. IEEE, 2013.

[7]   Felbinger, Jonathan G., M. V. S. Chandra, Yunju Sun, Lester F. Eastman, John Wasserbauer, Firooz Faili, Dubravko Babic, Daniel Francis, and Felix Ejeckam. "Comparison of GaN HEMTs on Diamond and SiC substrates." Electron Device Letters, IEEE 28, no. 11 (2007): 948-950.

[8]   Element Six. GaN-on-Diamond Heat Spreader. [ONLINE] Available at: http://www.e6.com/wps/wcm/connect/E6_Content_EN/Home/Applications/Electronics/Thermal/GaN-on-Diamond/. [Accessed 26 October 15].

[9]   Baltynov T, Unni V, Narayanan EM. The world's first high voltage GaN-on-diamond power devices. In Solid State Device Research Conference (ESSDERC), 2015 45th European 2015 Sep 14 (pp. 126-129). IEEE.

[10]   Zhang, Naiqian, Vivek Mehrotra, Sriram Chandrasekaran, Brendan Moran, Likun Shen, Umesh Mishra, Edward Etzkorn, and David Clarke. "Large area GaN HEMT power devices for power electronic applications: switching and temperature

characteristics." In Power Electronics Specialist Conference, 2003. PESC'03. 2003 IEEE 34th Annual, vol. 1, pp. 233-237. IEEE, 2003.

[11] Lin, Yu-Syuan, Jia-Yi Wu, Chih-Yuan Chan, Shawn SH Hsu, Chih-Fang Huang, and Ting-Chi Lee. "Square-gate AlGaN/GaN HEMTs with improved trap-related characteristics." Electron Devices, IEEE Transactions on 56, no. 12 (2009): 3207-3211.

[12] Raj, Balwant, and Sukhleen Bindra. "Thermal Analysis of AlGaN/GaN HEMT: Measurement and Analytical Modeling Techniques." Int. J. Comput. Appl 75 (2013): 4-13.

[13] Tanaka, Kenichiro, Masahiro Ishida, Tetsuzo Ueda, and Tsuyoshi Tanaka. "Effects of deep trapping states at high temperatures on transient performance of AlGaN/GaN heterostructure field-effect transistors." Japanese Journal of Applied Physics 52, no. 4S (2013): 04CF07.

[14] As, Donat J., Alexander Zado, Qiyang Y. Wei, Ti Li, Jingyi Y. Huang, and Fernando A. Ponce. "Capacitance Voltage Characteristics and Electron Holography on Cubic AlGaN/GaN Heterojunctions." Japanese Journal of Applied Physics 52, no. 8S (2013): 08JN04.

[15] Reeves, G. K., and H. B. Harrison. "Obtaining the specific contact resistance from transmission line model measurements." Electron Device Letters, IEEE 3, no. 5 (1982): 111-113.

[16] Ardali, S., G. Atmaca, S. B. Lisesivdin, T. Malin, V. Mansurov, K. Zhuravlev, and E. Tiras. "The variation of temperature-dependent carrier concentration and mobility in AlGaN/AlN/GaN heterostructure with SiN passivation." physica status solidi (b) 252, no. 9 (2015): 1960-1965.

FIGURES
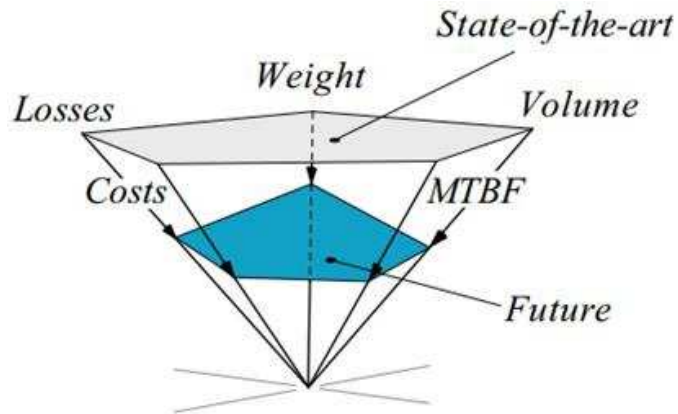
Fig. 1: Development trends in power converters [1].
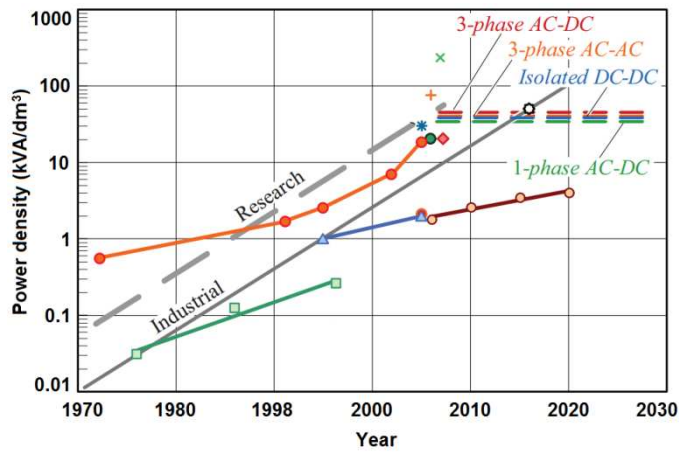
Fig. 2: Power density trend of industrial and research systems and the Power Density Barriers [1].
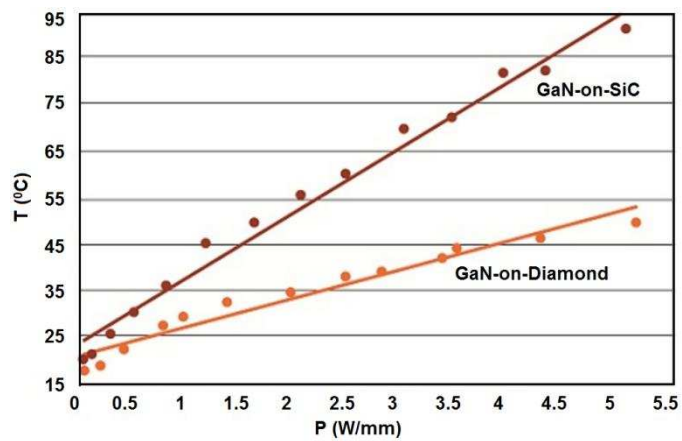

Fig. 3: Peak channel temperatures of GaN-on-Diamond and GaN-on-SiC HEMTs [8].
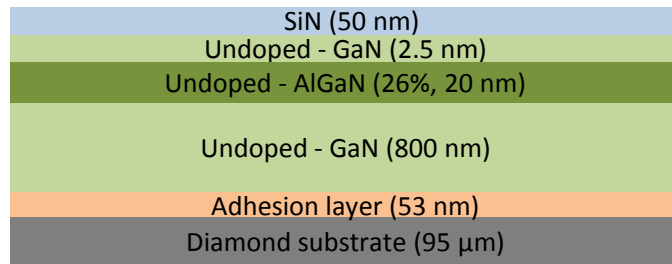
Fig. 4: Epi-layer structure of GaN-on-Diamond substrate supplied by Element Six.
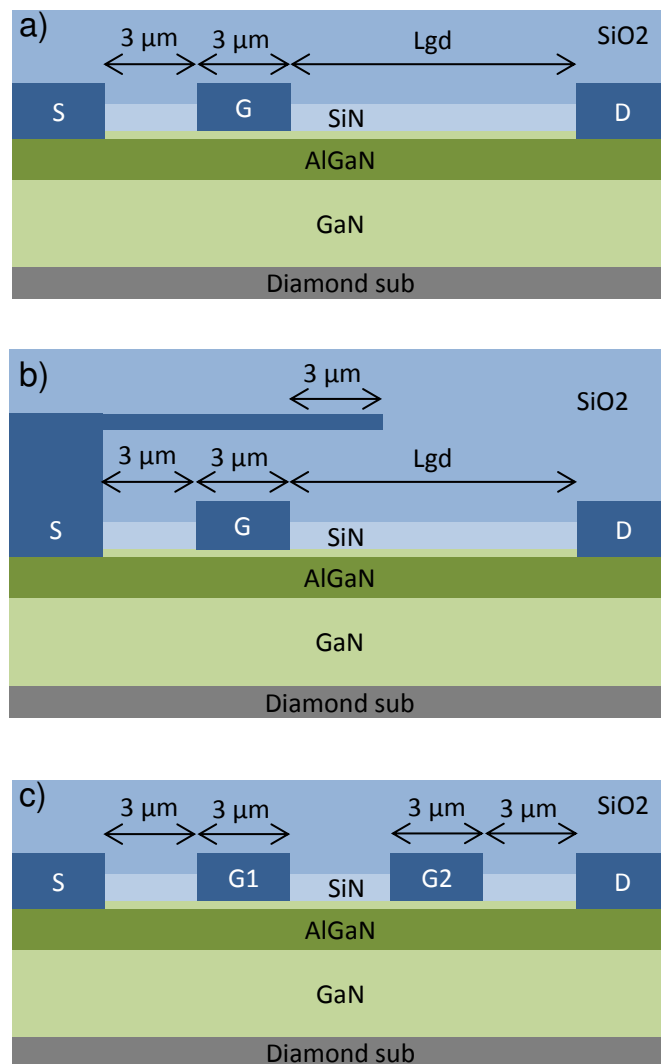
Fig. 5: Cross-sectional schematics of (a) AlGaN/GaN HEMT (without FP), (b) AlGaN/GaN HEMT (with SFP), and (c) bidirectional AlGaN/GaN HEMT.
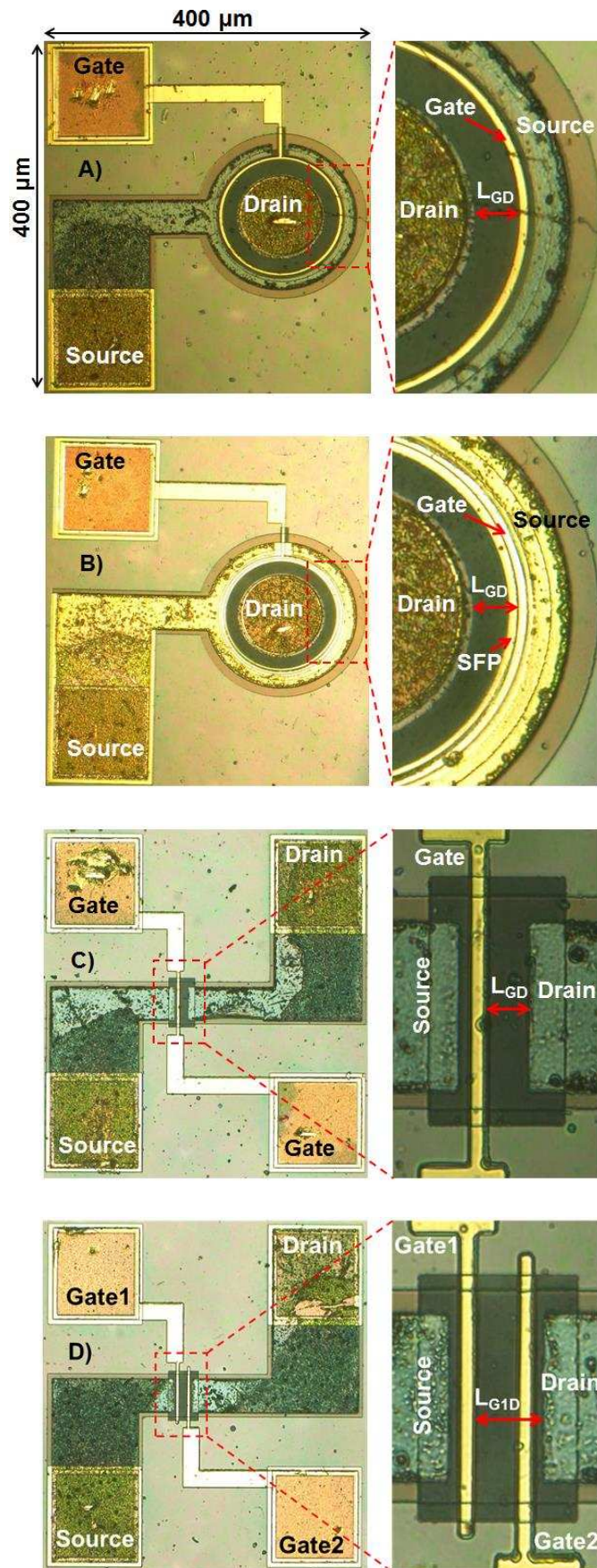
Fig. 6: Top view photographs of the fabricated AlGaN/GaN HEMTs (a) circular (without FP), (b) circular (with SFP), (c) stripe form (without FP), and (d) bidirectional.
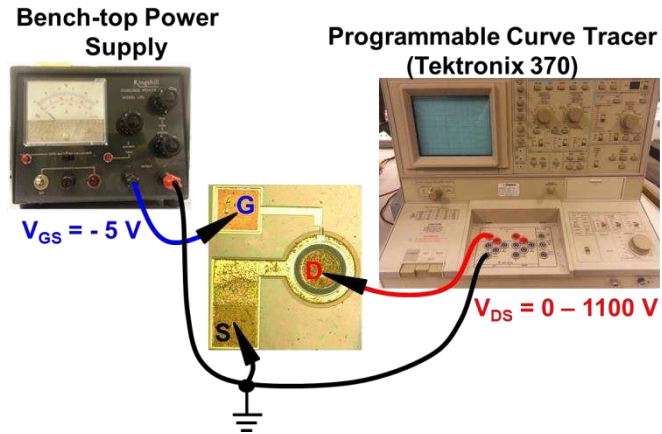
Fig. 7: Simplified illustration of the setup for breakdown voltage measurements.
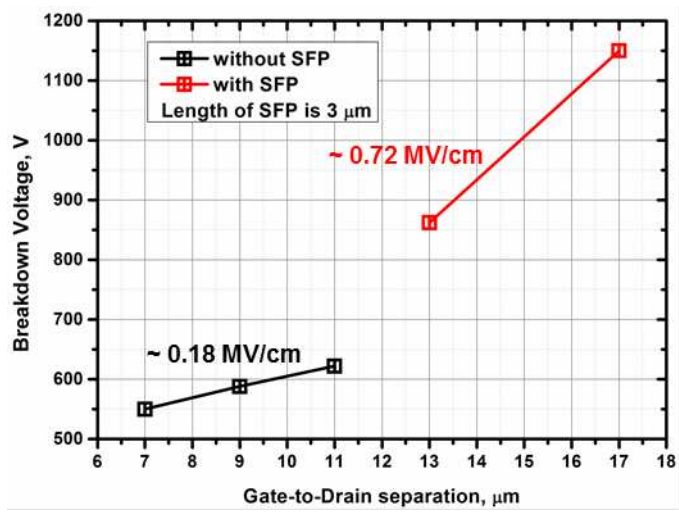
Fig. 8: Breakdown voltage versus gate-to-drain separation.
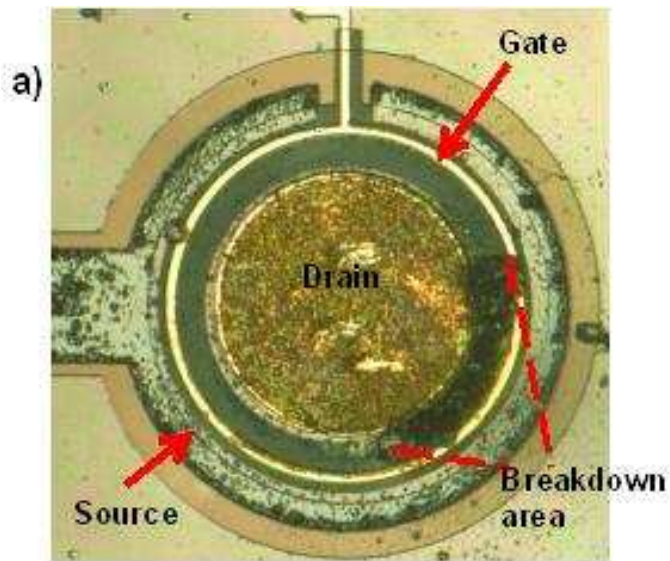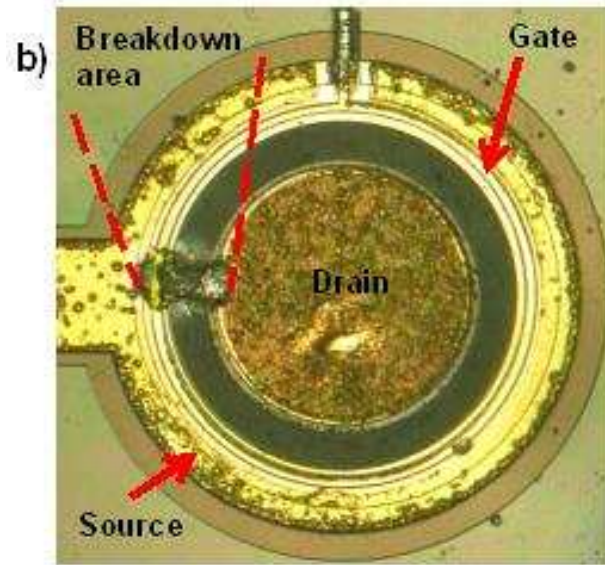
Fig. 9: Top view photographs of circular AlGaN/GaN HEMTS post breakdown tests (a) without source field plate and L_{GD} = 11 μm (b) with source field plate and L_{GD} =17 μm (BV$_{DSS}$ ~ 1100 V).
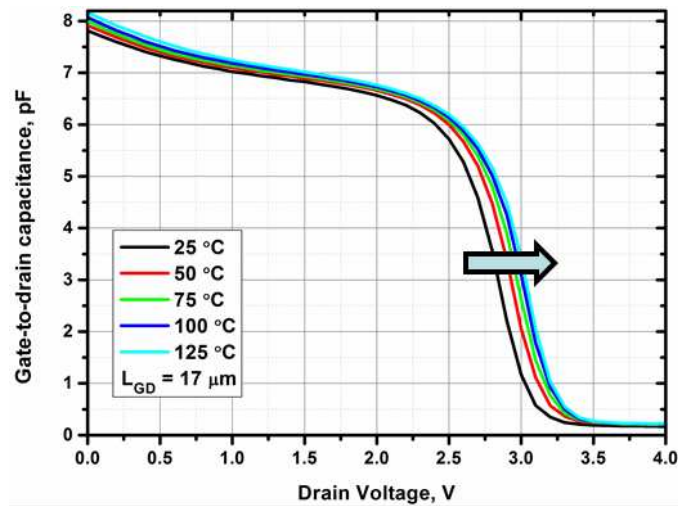
**Fig. 10:** Capacitance – voltage (CV) characteristics of a high voltage circular AlGaN/GaN HEMT performed at various temperatures.
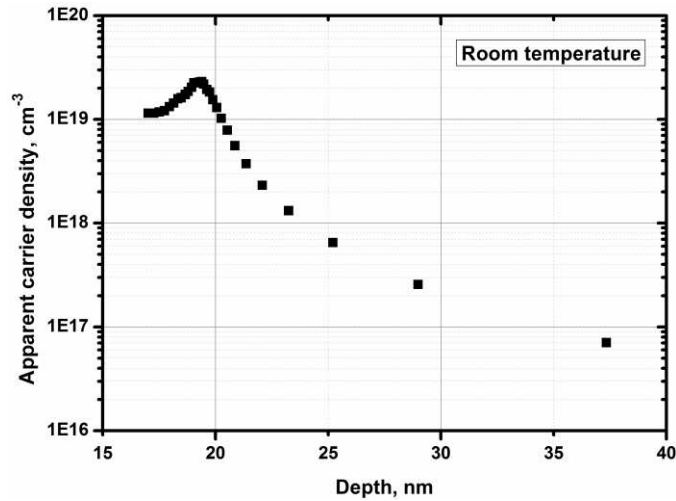
Fig. 11: Extracted apparent carrier density profile in a high voltage circular AlGaN/GaN HEMT, based on CV characteristics
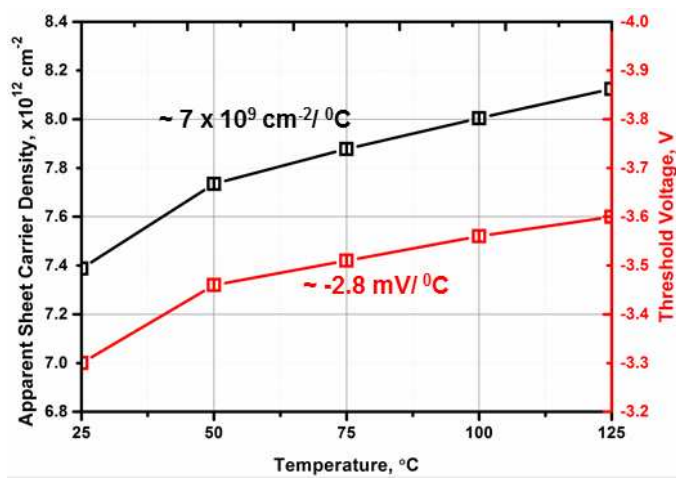

Fig. 12: Variation of the apparent sheet carrier concentration and Threshold Voltage (V_{TH}) with respect to temperature, as extracted from CV characteristics.
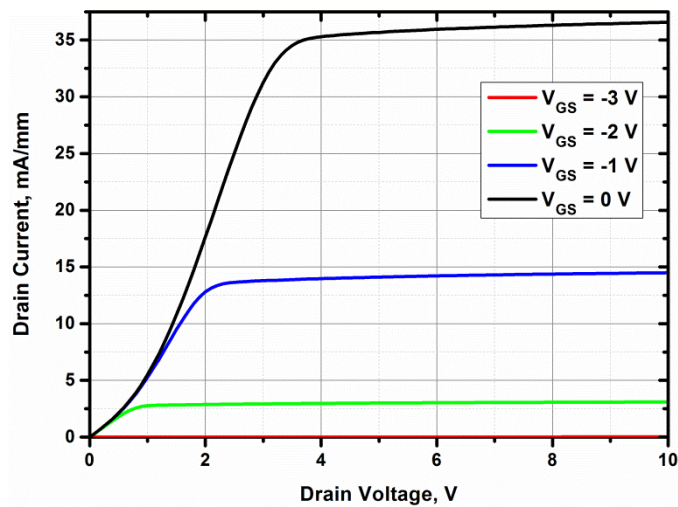

Fig. 13: Output I – V characteristics of a high voltage circular AlGaN-GaN HEMT with W_G = ~420 μm, L_{GD} = 17 μm and L_{SFP} = 3 μm.
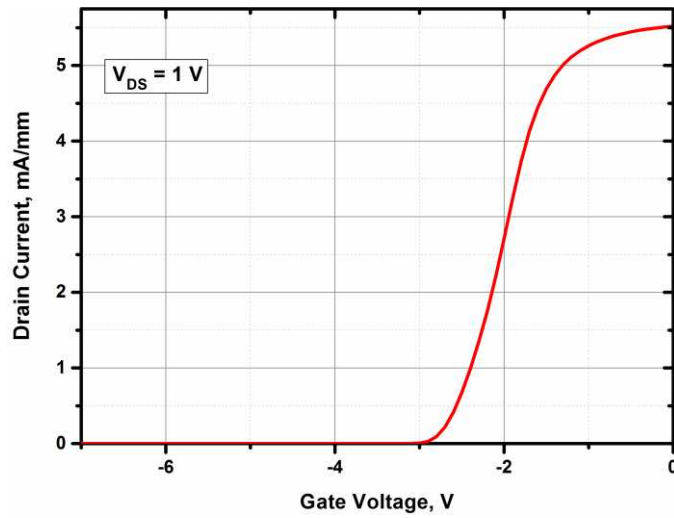
Fig. 14: Transfer I – V characteristics of a high voltage circular AlGaN/GaN HEMT with W_G = ~420 μm, L_{GD} = 17 μm and L_{SFP} = 3 μm.
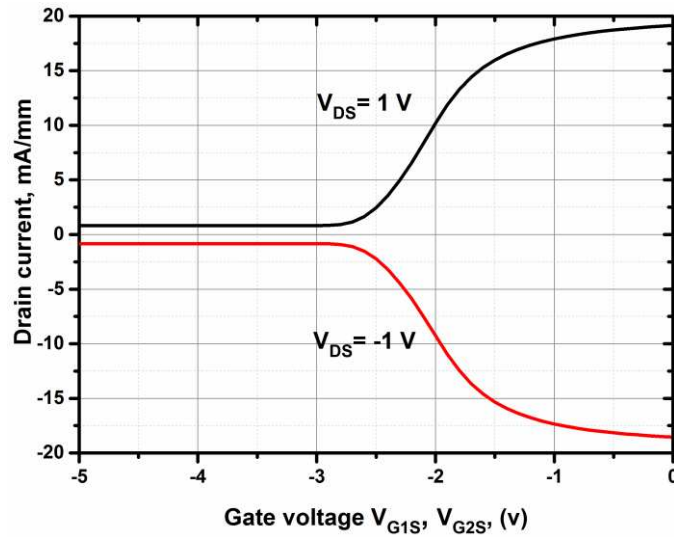

Fig. 15: Transfer I – V characteristics of a bidirectional AlGaN/GaN HEMT with $L_{G1D} = L_{G2S}$ = 17 μm, L_{G1} = L_{G2} = 3 μm, and $W_{G1} = W_{G2}$ = 50 μm.
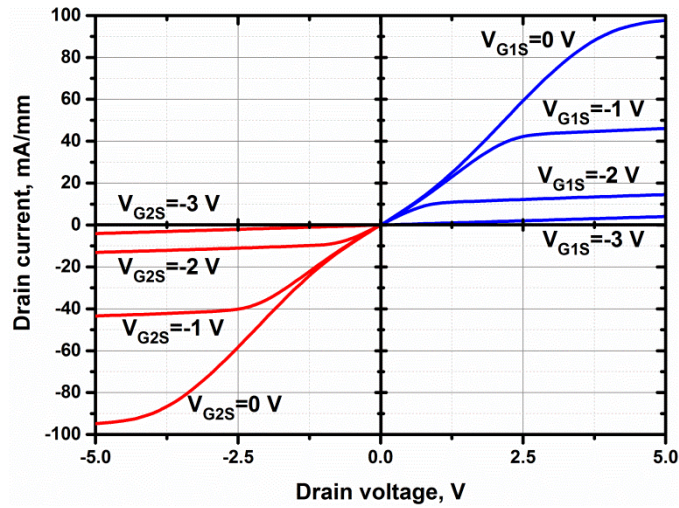
Fig. 16: Transfer I – V characteristics of a bidirectional AlGaN/GaN HEMT with $L_{G1D} = L_{G2S} = 17$ μm, $L_{G1} = L_{G2} = 3$ μm, and $W_{G1} = W_{G2} = 50$ μm.
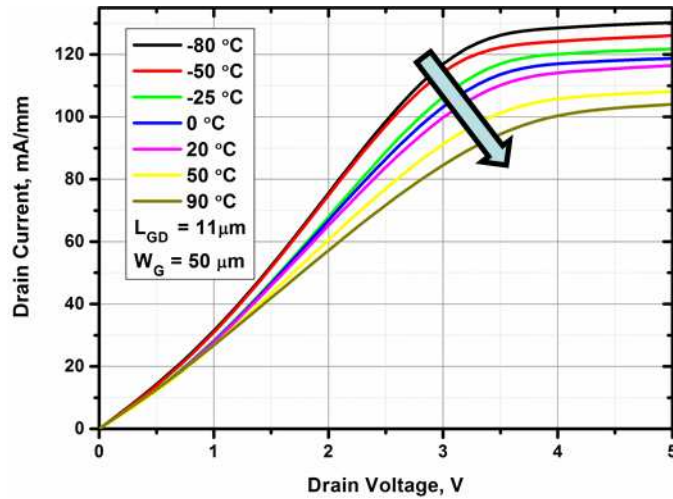
Fig. 17: Output I-V of a linear AlGaN/GaN HEMT (without field plate) with respect to temperature ($V_{GS} = 0$ V).
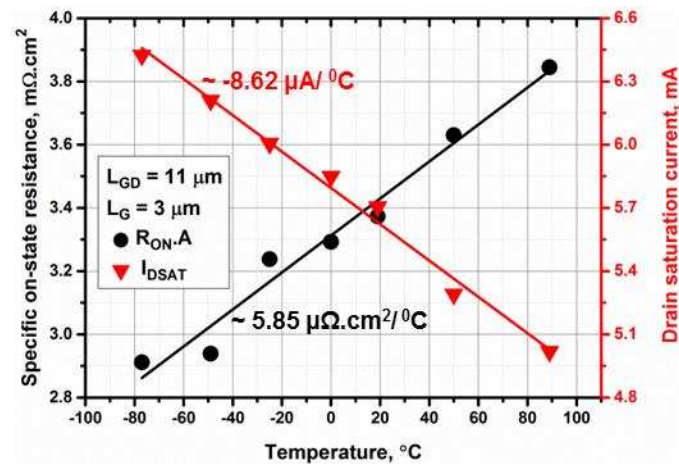
Fig. 18: Specific on-state resistance (at $V_{DS} = 2V$ and $V_{GS} = 0V$) and drain saturation current (at $V_{DS} = 4V$ and $V_{GS} = 0V$) of a conventional AlGaN/GaN HEMT (without field plate) with respect to temperature.